

Numerical Study of the Entrance Effects in an Oscillatory Flow of a Standing-Wave Thermoacoustics

Open
Access

Siti Hajar Adni Mustaffa¹, Fatimah Al-Zahrah Mohd Saat^{1,2,*}, Ernie Mattokit¹

¹ Faculty of Mechanical Engineering Universiti Teknikal Malaysia Melaka, Hang Tuah Jaya, 76100 Durian Tunggal, Melaka, Malaysia

² Centre of Advanced Research on Energy, Universiti Teknikal Malaysia Melaka, Hang Tuah Jaya, 76100 Durian Tunggal, Melaka, Malaysia

ARTICLE INFO

ABSTRACT

Article history:

Received 5 February 2018

Received in revised form 6 March 2018

Accepted 7 March 2018

Available online 24 March 2018

Entrance effect and formation of the vortex structure play a vital role in understanding the flow physics at the channel entry especially in oscillatory flow inside the channel between thermoacoustic stack plates. The aims of the current study are to investigate the effect of flow frequency on the structure of the vortex shedding at the end of the stack plates and also the effect of the vortex formation at the end of the plates associated with “entrance effect”. The methods used are CFD simulation with ANSYS FLUENT as a solver. The flow was solved using laminar model and two-equation Shear-Stress Transport (SST) $k-\omega$ turbulence model. The “entrance effect” and vortex flow phenomena has been studied for two drive ratios, DR (defined as ratio of maximum pressure amplitude to mean pressure) which are 0.65% and 1.0% at two frequencies of 13.1 Hz and 23.1 Hz. The results shows that at higher frequency, the entrance length becomes shorter. This can be emphasized that flow frequency plays a significant role as it affected the entrance length and vortex formation and structure of the flow.

Keywords:

Oscillatory flow, entrance region,
turbulence, standing-wave,
thermoacoustics

Copyright © 2018 PENERBIT AKADEMIABARU - All rights reserved

1. Introduction

Since the breakthrough of potential energy in sound which was made by Byron Higgins in 1777, who first observed the heat induced acoustic oscillations, many researchers have now turn their interest into a technology called thermoacoustics. Thermoacoustics is a technology that can be used to produce power or energy system by harnessing energy from sound. The basis of thermoacoustic principle is an interaction between sound wave and solid surface inside an environment which at the correct setting would produce either power (heat engine) or cooling effect (refrigerator). This technology offers an alternative green technologies due to the lack of moving parts in the thermodynamic process, which makes them simple, reliable and low cost [1]. Examples of thermoacoustics systems may be found in [2-4]. In thermoacoustics, the flow that govern the system are called oscillatory flow. Oscillatory flow is a cyclic flow where the fluid is

* Corresponding author.

E-mail address: fatimah@utem.edu.my (Fatimah Al-Zahrah Mohd Sa'at)

flowing in bidirectional ways as it moves in forward and reverse directions. The unique behaviour of flows require special attention because the fluid dynamics phenomena such as turbulence [5,6], vortex shedding [7,8], thermal-driven flow [9,10], friction losses [11] and streaming [12] are not behaving exactly the same as the conventional unidirectional flow. For instance, modelling turbulence in the conventional unidirectional flow in itself is already a challenge when new fluids (i.e. nanofluids) are used in the system [13,14]. This condition could be complicated further should the newly introduced fluids are used in systems with oscillatory flow.

The oscillation of flow into and out of any channel could also alters the fluid behaviour in that channel. The development of the flow at the channel entry, which is also known as “entrance effects”, associated with turbulent transition has become a subject of study in thermoacoustics as it affects the behaviour of the oscillatory flow caused by discontinuities of the cross-sectional area of the important components of the system such as stacks, regenerators and heat exchangers. Yamanaka *et al.*, [15] defined the “entrance effect” for unidirectional pipe flow and it is described as the region where the transition from a uniform velocity profile to the fully developed profile takes place. In unidirectional flow, the entrance effect is very much relying on the velocity that represents the speed of flow. In thermoacoustics, the fluid flows is bidirectional. An important parameter that is often used in representing thermoacoustic’s amplitude of flow is known as a drive ratio, DR. The drive ratio is defined as a ratio of maximum pressure amplitude to the mean pressure. Jaworski and his co-worker [16] studied vortex formation and shedding and also the “entrance length” during the suction phase; when the fluid enters the channel from outside using the combination of experimental data obtained from PIV and CFD solutions. They defined the equation for “entrance length” as a function of time (or phase), as follows:

$$u(L(t),0,t) - u(\infty,0,t) = 0.01nu_{ref} \quad (1)$$

where n is a “tolerance number” and u_{ref} is a reference velocity. They revealed the “entrance length”, in normalised term, as equal to 2.29 (based on equation (1)). Equation (1) was derived based on results taken at the DR = 0.3%, for the plate thickness = 5 mm and plate spacing = 10 mm. However, their studies only reported the entrance length at DR = 0.3%. The flow at DR = 0.3% may be treated as laminar. Earlier investigation have reported that turbulence may starts at drive ratio as early as 0.45%. Turbulence may alters the entrance region and therefore further investigations are needed here.

In the classical fluid dynamics analysis of unidirectional flow inside a pipe, entrance length equation was defined based on whether the flow is laminar or turbulence. These two conditions of “entrance region” are described in equations (2) and (3) [17]:

$$L_h \text{ (laminar)} \approx 0.05ReD \quad (2)$$

$$L_h \text{ (turbulent)} \approx 10D \quad (3)$$

The terms Re and D in equations (2) and (3) are the Reynolds number and the diameter of the pipe. The diameter is the characteristic length that represents the hydraulic diameter for pipe. Depending on the type of flow, equations (2) and (3) may be used to estimate entrance length for flow inside an object/channel/pipe.

The motivation for current study is to understand the behaviour of oscillatory flow at higher drive ratios and the “entrance effects” related to that conditions. Entrance effect was quite established for unidirectional flow. However, as fluid flows in bi-directional, the entrance effect

may be altered. In oscillatory flow, the study of entrance effect was reported in [16] but that was only for one drive ratio that represents laminar condition. The results reported in this paper is an extension of study that involves higher drive ratios and an increase of flow frequency.

2. Methodology

In the current numerical study, two-dimensional (2D) computational domain is developed using ANSYS FLUENT software based on the experimental rig built at Universiti Teknikal Malaysia Melaka [18]. Figure 1 shows the computational domain, the enlarge view of the stack area and the definition of phases in one flow cycle. The computational domain was built at 600 mm length and 144.4 mm width as shown on top of Figure 1. A larger view of the parallel-plates stack (only 3 plates shown) was also shown in Figure 1. Each plate is 3.0 mm thick (d), 200 mm long (l) and the plates are evenly-spaced with gap between each plate, $D = 6$ mm. The plates are made of Aluminium. In standing-wave thermoacoustic systems, the stack is placed at 0.17λ from the pressure antinode at the end of the resonator so that a better thermoacoustic effect can be gained.

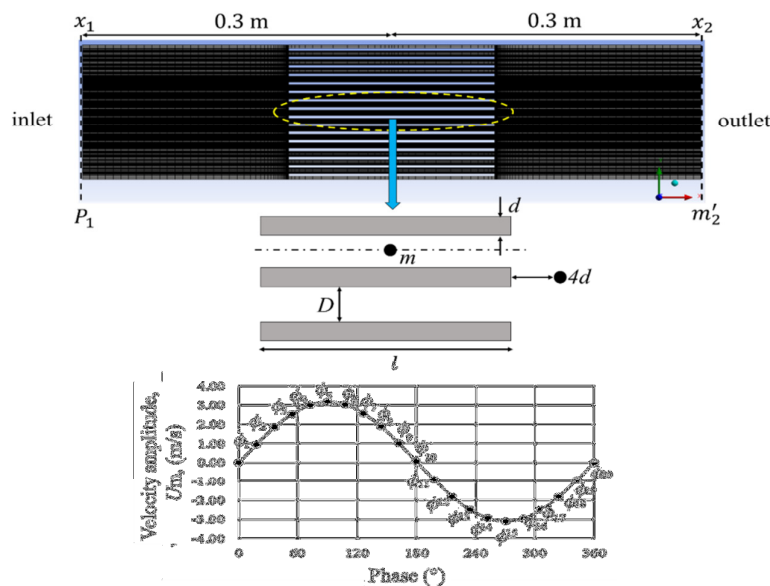


Fig. 1. Schematic diagram of the computational domain (top) the enlarge view of geometry of the stack (middle, with only three plates shown as illustration) and the oscillatory flow defined in twenty phases (bottom)

In this study, the models has been solved for two flow frequencies of 13.1 Hz and 23.1 Hz. The wavelength depends on frequency so does the stack's location. Hence for a fair comparison between studies, the stack has been placed both at 0.17λ which corresponds to the distance of 4.5 m and 2.6 m from the pressure antinode for frequencies of 13.1 Hz and 23.1 Hz, respectively. At this two locations, the flow amplitude within the quarter standing wavelength resonator are theoretically the same. As for requirement for standing-wave thermoacoustic systems, the pressure and velocity was set 90° out of phase. The mean pressure was set to 0.1 MPa. The working medium is air at atmospheric pressure and room temperature and was modelled as an ideal gas. Data are recorded in 20 phases (ϕ_1 to ϕ_{20}) of a flow cycle as illustrated at the bottom of Figure 1. The first ten phases (ϕ_1 to ϕ_{10}) represent forward direction of flow while the last ten phases (ϕ_{11} to ϕ_{20}) represent the reversed flow.

The flow was modelled using Navier-Stokes equation for laminar model and Reynolds-averaged Navier-Stokes (RANS) equation for turbulence model [19]. The RANS turbulence model chosen in this study is a two-equation Shear Stress Transport (SST) $k-\omega$ turbulence model as suggested in [6]. The unsteady models were solved using a time step size of $1/1200f$ and each solution was monitored until convergence takes place at every time step. The pressure-based solver with the applications of Pressure-Implicit with Splitting Operators (PISO) scheme for the pressure-velocity coupling was selected. The PISO scheme was chosen because it provides faster convergence for unsteady flow cases.

Table 1 shows the boundary conditions for cases reported in this work. The boundary conditions were calculated using lossless equations of quarter-wavelength device [6]. As shown in Figure 1, oscillating pressure, P_1 , is placed at the inlet, at x_1 location, while oscillating mass flux, m'_2 , is placed at the outlet, at x_2 location. For turbulence model, additional parameters such as turbulent intensity, $I = 0.16(\text{Re})^{-1/8}$ and turbulent length scale, $\ell = 0.07D$ are assigned at the boundaries. The Reynolds number, defined as $\text{Re} = \rho U D / \nu$, where ρ is a density, U is a velocity, D is a gap spacing between plate and ν is a viscosity. The velocity, U , was obtained from theoretical calculations for both frequencies.

Table 1
 Boundary conditions

| Frequency, f (Hz) | Drive ratio, DR (%) | Oscillating pressure, P_1 (Pa) | Oscillating mass flux, m'_2 (kg/m ²) |
|---------------------|---------------------|----------------------------------|--|
| 13.1 | 0.65 | 351.68 | 1.7084 |
| | 1.0 | 541.03 | 2.6284 |
| 23.1 | 0.65 | 370.22 | 1.7619 |
| | 1.0 | 569.57 | 2.7107 |

The model has been tested at three different grid sizes which are 59880, 78780 and 97680 cell counts. The type of meshing used in this study is quadrilateral structured mesh. As shown in Figure 1, the mesh was made denser near the plate's surface to capture boundary layer effects. The quadrilateral mesh was designed with a growth ratio of 1.2. The smallest mesh was recorded with the size of 0.21 mm. It was found that 78780 number of cell counts (corresponding to a $y^+ = 0.98$) is sufficient enough to solve the flow solutions. The quality mesh can also be presented in terms of orthogonal quality (close to one for good quality) and skewness factors (close to zero for good quality). The minimum orthogonal quality for the current model is 0.95 and the maximum skewness is 1.31×10^{-10} , which show that the mesh is in good quality conditions. Data are processed after steady oscillatory flow condition is achieved (i.e. oscillating pressure and velocity are not changing with oscillation cycle).

3. Results and Discussion

3.1 Validation with Experimental Data

The values of axial velocity, U_e (m/s), at the location $4d$ (where d is a thickness of the plate as shown in Figure 1) has been obtained from numerical models. The data has been validated with theoretical and experimental data at the same exact location. The experimental data was collected using experimental rig reported in [18] and the theoretical solution was based on the the Rott's linear equation [20]. The porosity (defined as the cross-sectional area of the stack occupied by the plates over the cross-sectional area of the resonator) at the location of $4d$ where axial velocity, U_e

(m/s), was measured is 100%. Figure 2 shows the plotted graph of axial velocity against drive ratios. The values of axial velocity from SST $k-\omega$ turbulence model and laminar model falls in-line with the theoretical and experimental data. Hence, this shows that the data obtained from current numerical works is validated with the theoretical and experimental data for all investigated drive ratios reported here. It is noteworthy that as the drive ratios increase the axial velocity also increase.

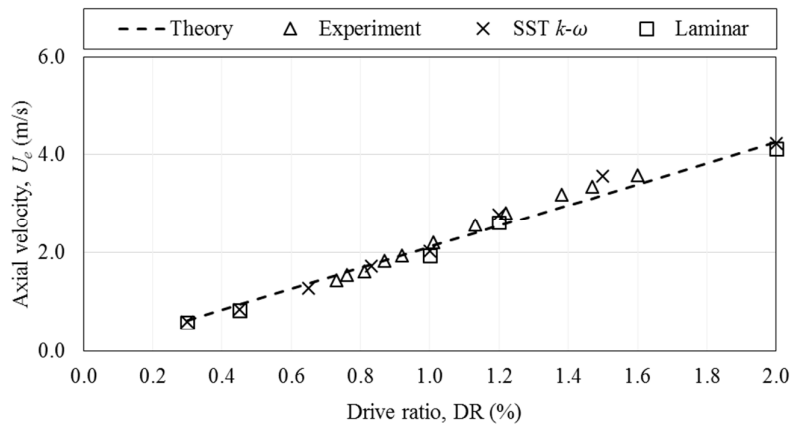


Fig. 2. Validation of the numerical values of axial velocity with measured experimental data

3.2 Vortex Plot

Figure 3 and Figure 4 show results of CFD simulations for forward flow at phases, ϕ_1, ϕ_3, ϕ_5 and ϕ_8 while phases, $\phi_{11}, \phi_{13}, \phi_{15}$ and ϕ_{18} represent reverse flow. The vorticity plot is used for flow visualization as means of showing the vortex formation and shedding at the end of the plates in oscillatory flow conditions for both flow frequencies.

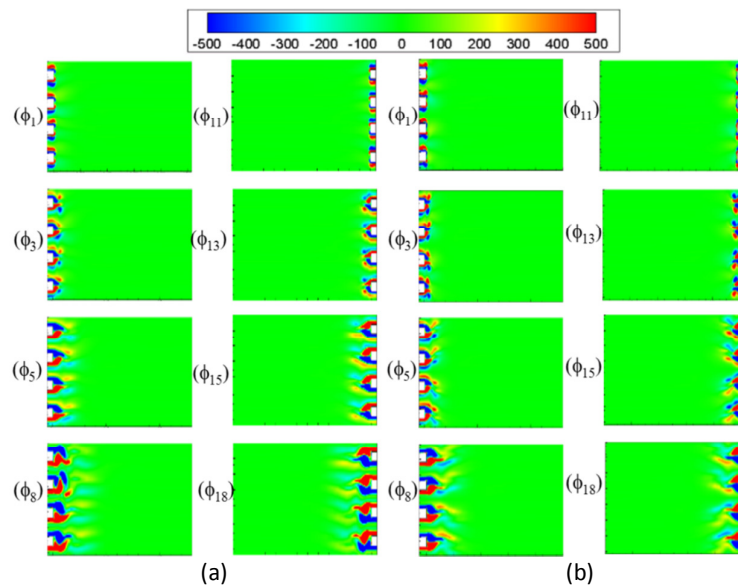


Fig. 3. Vorticity fields for the flow at the end of the stack using laminar model at drive ratio, DR = 0.65% at frequencies, f , (a) 13.1 Hz ($Re_\delta = 119$), (b) 23.1 Hz ($Re_\delta = 88$). Scale of vorticity, s^{-1}

In oscillatory flow, the fluid flows forward during the first part of the cycle, while the flow reversed in the latter part of the cycle. The simulation results discussed here are taken for the drive ratios of $DR = 0.65\%$ and $DR = 1.0\%$ at both flow frequencies, which are $f = 13.1$ Hz and $f = 23.1$ Hz. At $DR = 0.65\%$, the velocity amplitude at the middle of the stack, U_m , for both frequencies, f ; 13.1 Hz and 23.1 Hz are 2.33 m/s and 2.30 m/s respectively. While, at $DR = 1.0\%$, the corresponding velocity amplitude at the middle of the stack, U_m , for f ; 13.1 Hz and 23.1 Hz are 3.75 m/s and 3.48 m/s respectively. The comparison of vortex structures are made for the same drive ratio of 0.6%. The slight difference of velocity amplitude between the two frequencies may be due to the effect of frequency where particle of gaseous flows in a more rapid movement as frequency becomes higher. There may be some friction losses involved, hence the mean velocity tend to be slightly lower. This friction losses may also be related to the vortex structure change that can be seen for the two flow frequencies.

Generally, Figures 3 and 4 show that as velocity increases from ϕ_1 to ϕ_8 the vortex structure at the end of plates becomes longer. These structures are then sucked back into the channel as the fluid reverses its direction (as shown for ϕ_{11} to ϕ_{18}). At maximum flow velocity, shown here as ϕ_8 , the vortex at the end of plates for frequency 13.1 Hz shows a sign of 'wiggle' and 'breakage'. This is not clearly seen for frequency of 23.1 Hz. However, the secondary layer of vortex are more prominent for the flow with high frequency. The vortex sheds at the end of the stack plates in Figure 4 is solved using SST k- ω turbulence model. At higher drive ratio, (shown here as $DR=1\%$ in Figure 4), the vortex structure at the end of plates are longer than the flow with low drive ratio. In the beginning of the cycle in Figure 4, the vortex appears symmetrically for both frequencies. The "two vortices" flow phenomena only appear at low frequency, while "four vortices" flow phenomena seems more significant at higher frequency. The flow boundary layer for low frequency seem to experience faster 'breakage' compared to the higher frequency. At the higher frequency, the vortex starts to elongate until reverse flow takes place as the flow is being sucked back into the channel. This vortex shedding flow pattern phenomena might influence the entrance region and the associated boundary layer inside the channel between plates.

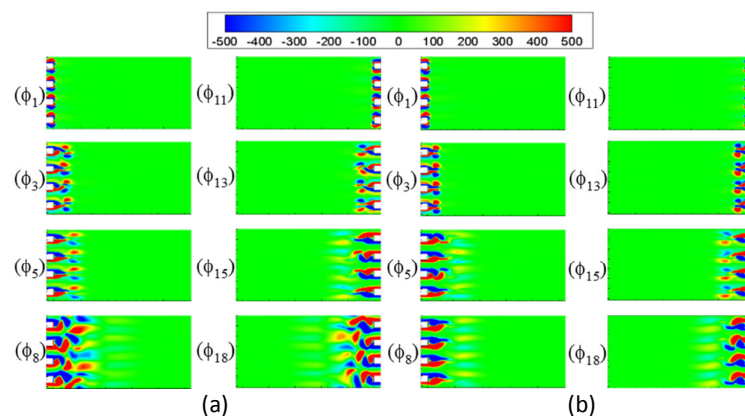


Fig. 4. Vorticity fields for the flow at the end of the stack using SST k- ω turbulence model at drive ratio, $DR = 1\%$ at frequencies, f , (a) 13.1 Hz ($Re_\delta = 191$), (b) 23.1 Hz ($Re_\delta = 132$). Scale of vorticity, s^{-1}

In oscillatory flow, fluid flows back and forth in cyclic manner. Hence, the vortex structures at the end of plates will be sucked back following that cyclic change of the flow. This will alters the behaviour of fluid flows within the channel of the plates. Hence, the investigation of flow within the channel is presented in the next section.

3.3 Entrance Region

The “entrance region/ length” is a region (or length) where the velocity profile is changing until it reached a “fully developed flow” where the velocity profile remains constant. Jaworski et al. [16] defined the “entrance length” as the distance from the channel entry to the point where centreline velocity deviates 1% from the fully developed profile. This definition of the “entrance length” have been adopted in the current study as a way to identify the length of the “entrance region”. Figures 5(a) – 5(d) shows the plotted graph of the distribution of velocity amplitude at the centre of the channel for DR = 0.65% and DR = 1% at low flow frequency ($f = 13.1$ Hz) and high flow frequency ($f = 23.1$ Hz).

The “wavy pattern” as can be seen in all plotted graph in Figures 5(a) until 5(d) reveals the extent of the “entrance length” phase-by-phase. Interestingly, it is found that the “wavy pattern” in phase ϕ_{20} having the “entrance region” extends the furthest into the channel for all cases in the current study. This is the phase where the reverse flow is at its maximum amplitude and the flow is about to change its’ direction. Thus the ‘wavy pattern’ appearing in ϕ_{20} is not only representing the effect of the ‘sucked’ vortices but also the effect of the reversing nature of particles that happens at all levels and locations of the channel.

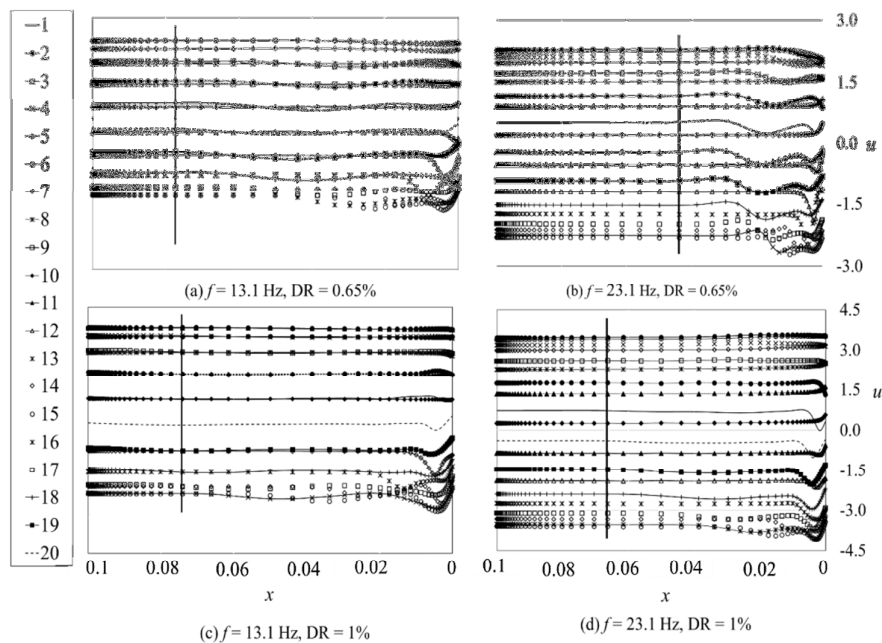


Fig. 5. Distribution of velocity amplitude at the centre of the channel for DR = 0.65% (a) $f = 13.1$ Hz, (b) $f = 23.1$ Hz and DR = 1%, (c) $f = 13.1$ Hz, (d) $f = 23.1$ Hz. The results are plotted for all twenty phases in the flow cycle. The vertical line serves as a guide for entrance length

Figure 5 also shows that the entrance length for low frequency (Figure 5 (a) and (c)) is longest compared to the higher frequency (Figure 5 (b) and (d)). This might be related to the rapidness of flow. At low frequency, the fluid flows to a longer distance and the time taken to complete one cycle is long. At high frequency, fluid flows in a more rapid nature where the air particles travel to a shorter distance and the cycle is completed in a shorter period. Hence, the entrance length tends to be shorter as the frequency increases.

The model was then solved for additional flow frequencies. The results for entrance length for all cases including a few additional cases that were considered in the current work is summarised as shown in Table 2. Evidently, the entrance length is longer as Reynolds number (related to drive ratio) increases. The prediction of entrance length following the classical equations (2) and (3) as defined earlier is also shown in the last column of Table 2. In the calculation, the size of gap between channels, D , was used as it represents the size of the channel. Comparison between the current results ($X_{entrance}$) and the prediction from classical text books ($X_{equations (2) \text{ and } (3)}$) shows a very huge different particularly for low drive ratio where the flow is to be treated as laminar. At higher drive ratios, the theoretical predictions give values slightly lower than the results of the validated numerical models. The deviation becomes bigger as drive ratio increases. The results shown here indicate that the classical equation for predicting entrance region may not be so suitable to be used for estimating entrance region of an oscillatory flow condition found in many thermoacoustic devices.

Table 2
 Entrance length based on drive ratios and flow frequencies

| Frequency, f (Hz) | Drive ratio, DR (%) | Velocity amplitudes at the middle of the stack, U_m (m/s) | Reynolds number, Re | $X_{entrance}$ (m) | $X_{equations (2) \text{ and } (3)}$ (m) |
|------------------------|------------------------|---|------------------------|-----------------------|---|
| 13.1 | 0.65 | 2.33 | 1040 | 0.0801 | 0.3121 |
| | 0.83 | 2.97 | 1326 | 0.0704 | 0.3978 |
| | 1.0 | 3.75 | 1674 | 0.0741 | 0.06 |
| | 2.0 | 7.62 | 3402 | 0.0801 | 0.06 |
| | 3.0 | 11.58 | 5170 | 0.0826 | 0.06 |
| 23.1 | 0.65 | 2.30 | 1027 | 0.0561 | 0.3081 |
| | 0.83 | 2.98 | 1331 | 0.0615 | 0.06 |
| | 1.0 | 3.48 | 1554 | 0.0662 | 0.06 |
| | 2.0 | 7.31 | 3264 | 0.0704 | 0.06 |
| | 3.0 | 11.12 | 4965 | 0.0773 | 0.06 |

4. Conclusion

This paper presents an investigation of the vortex formation/shedding and entrance region (or length) at varied drive ratios and flow frequencies for an oscillatory flow in thermoacoustics. There are several significant findings that can be concluded from the current study: (i) at frequency of 13.1 Hz, the structure of the vortex shedding at the end of the plates shows a sign of ‘wobble’ and ‘breakage’, whereas this same flow structure are not justified for frequency of 23.1 Hz, (ii) for all cases studied, it is found that the change of flow direction and the “wavy pattern” of vortex mostly found in phase ϕ_{20} would lead to the extension of the “entrance region” further into the channel, and (iii) the entrance length becomes shorter as the flow frequency increases. The current study highlights that the cyclic nature of the flow has certain influence on the flow behaviour and it must be remembered that entrance region may need to be defined on both sides (inlet and exit points) of the channel. In oscillatory flow, fluid flows back and forth in cyclic nature hence the fluid dynamics behaviour of flow must be analysed carefully with consideration of additional features that may not be described in conventional unidirectional flow.

Acknowledgements

This work is jointly supported by Ministry of Higher Education Malaysia (FRGS/1/2015/TK03/FKM/03/F00274) and Universiti Teknikal Malaysia Melaka (UTeM).

References

- [1] Zolpakar, Nor Atiqah, Normah Mohd-Ghazali, and Mawahib Hassan El-Fawal. "Performance analysis of the standing wave thermoacoustic refrigerator: A review." *Renewable and Sustainable Energy Reviews* 54 (2016): 626-634..
- [2] Zhang, S., Z. H. Wu, R. D. Zhao, G. Y. Yu, W. Dai, and E. C. Luo. "Study on a basic unit of a double-acting thermoacoustic heat engine used for dish solar power." *Energy Conversion and Management* 85 (2014): 718-726.
- [3] Sharify, Esmatullah Maiwand, and Shinya Hasegawa. "Traveling-wave thermoacoustic refrigerator driven by a multistage traveling-wave thermoacoustic engine." *Applied Thermal Engineering* 113 (2017): 791-795..
- [4] Abdoulla-Latiwish, Kalid OA, Xiaohan Mao, and Artur J. Jaworski. "Abdoulla-Latiwish, Kalid OA, Xiaohan Mao, and Artur J. Jaworski. "Thermoacoustic micro-electricity generator for rural dwellings in developing countries driven by waste heat from cooking activities." *Energy* 134 (2017): 1107-1120.
- [5] Mao, Xiaohan, and Artur J. Jaworski. "Application of particle image velocimetry measurement techniques to study turbulence characteristics of oscillatory flows around parallel-plate structures in thermoacoustic devices." *Measurement Science and Technology* 21, no. 3 (2010): 035403.
- [6] Mohd Saat, Fatimah AZ, and Artur J. Jaworski. "Numerical Predictions of Early Stage Turbulence in Oscillatory Flow across Parallel-Plate Heat Exchangers of a Thermoacoustic System." *Applied Sciences* 7, no. 7 (2017): 673.
- [7] Shi, Lei, Zhibin Yu, Artur J. Jaworski, and Abdulrahman S. Abduljalil. "Vortex shedding at the end of parallel-plate thermoacoustic stack in the oscillatory flow conditions." *World Academy of Science, Engineering and Technology* 49 (2009).
- [8] Mao, Xiaohan, Zhibin Yu, Artur J. Jaworski, and David Marx. "PIV studies of coherent structures generated at the end of a stack of parallel plates in a standing wave acoustic field." *Experiments in Fluids* 45, no. 5 (2008): 833-846.
- [9] Mohd Saat, Fatimah AZ, and Artur J. Jaworski. "The effect of temperature field on low amplitude oscillatory flow within a parallel-plate heat exchanger in a standing wave thermoacoustic system." *Applied Sciences* 7, no. 4 (2017): 417.
- [10] Shi, Lei, Zhibin Yu, and Artur J. Jaworski. "Application of laser-based instrumentation for measurement of time-resolved temperature and velocity fields in the thermoacoustic system." *International Journal of Thermal Sciences* 49, no. 9 (2010): 1688-1701.
- [11] Mohd Saat, Fatimah AZ, and Artur J. Jaworski. "Friction Factor Correlation for Regenerator Working in a Travelling-Wave Thermoacoustic System." *Applied Sciences* 7, no. 3 (2017): 253.
- [12] Matveev, Konstantin, Scott Backhaus, and Greg Swift. "On some nonlinear effects of heat transport in thermal buffer tubes." In *AIP Conference Proceedings*, vol. 838, no. 1, pp. 371-378. AIP, 2006.
- [13] Azwadi, CS Nor, and I. M. Adamu. "Turbulent force convective heat transfer of hybrid nano fluid in a circular channel with constant heat flux." *J. Adv. Res. Fluid Mech. Therm. Sci.* 19, no. 1 (2016): 1-9.
- [14] Abdulwahab, Mohammed Raad. "A numerical investigation of turbulent magnetic nanofluid flow inside square straight channel." *J. Adv. Res. Fluid Mech. Therm. Sci.* 1, no. 1 (2014): 44-52.
- [15] Yamanaka, G., H. Kikura, Y. Takeda, and M. Aritomi. "Flow measurement on oscillating pipe flow near the entrance using the UVP method." *Experiments in fluids* 34, no. 3 (2003): 307-315.
- [16] Jaworski, Artur J., Xiaohan Mao, Xuerui Mao, and Zhibin Yu. "Entrance effects in the channels of the parallel plate stack in oscillatory flow conditions." *Experimental Thermal and Fluid Science* 33, no. 3 (2009): 495-502.
- [17] Cengel, Yunus. *Heat and mass transfer: fundamentals and applications*. McGraw-Hill Higher Education, 2014.
- [18] S. H. A. Mustaffa., F. A. Z. Mohd Sa'at, E. Mat Tokit. "Design of experimental test-rig to investigate turbulence in oscillatory flow used in thermoacoustics." *Proceeding of Postgraduate Symposium on Green Engineering and Technology* (2016).
- [19] Versteeg, Henk Kaarle, and Weeratunge Malalasekera. *An introduction to computational fluid dynamics: the finite volume method*. Pearson Education, 2007.
- [20] Rott, Nikolaus. "Thermoacoustics." In *Advances in applied mechanics*, vol. 20, pp. 135-175. Elsevier, 1980.